Materials Science & Engineering C 94 (2019) 117–125

Contents lists available at ScienceDirect

Materials Science & Engineering C

journal homepage: www.elsevier.com/locate/msec

In vitro biocompatibility of new bioactive lithia-silica glass-ceramics

Juliana K.M.B. Daguano[a,*], Mariana T.B. Milesi[a], Andrea C.D. Rodas[a], Aline F. Weber[a], Jorge E.S. Sarkis[b], Marcos A. Hortellani[b], Edgar D. Zanotto[c]

[a] Grupo de Ciência e Tecnologia de Biomateriais, Centro de Engenharia, Modelagem e Ciências Sociais Aplicadas, Universidade Federal do ABC, São Bernardo do Campo, SP, Brazil
[b] Grupo de Caracterização Química e Isotópica, Instituto de Pesquisas Energéticas e Nucleares-IPEN-CNEN/SP, Universidade de São Paulo, São Paulo, SP, Brazil
[c] Laboratório de Materiais Vítreos, Departamento de Engenharia de Materiais, Universidade Federal de São Carlos, São Carlos, SP, Brazil

ARTICLE INFO

Keywords:
Bioactive glass-ceramic
Lithium disilicate
Crystallinity
In vitro biocompatibility
Bone regeneration
Dental applications

ABSTRACT

Glass-ceramics based on the Li_2O-SiO_2 system have been extensively used as restorative dental materials due to their excellent chemical durability, aesthetics, inertness in the buccal environment, and high fracture strength; but they are not bioactive. On the other hand, all known bioactive glasses show ability to bond to bone, teeth and cartilage coupled to osteoconduction and osteoinduction, but their fracture strength and toughness are rather low. The aim of this study is to develop and evaluate the *in vitro* biocompatibility of a new type of (bioactive and strong) lithia-silica glass-ceramic. For these purposes, two types of glass-ceramics based on a multicomponent lithia-silica system were studied: lithium metasilicate (LM) and lithium disilicate (LD). The *in vitro* bioactivity study was conducted in a SBF solution, before and after different times of immersion; the new materials were analyzed by XRD, FTIR, and SEM. Some samples were subjected to *in vitro* biodegradation tests to quantify the release of lithium and the weight loss. Cytotoxicity, adhesion, and cell proliferation on different samples were examined by using the Methyl Tetrazolium salt (MTS) and Alizarin Red. For ~40 vol% crystallinity, lithium metasilicate was detected as the major phase, whereas for ~80 vol% crystallinity, lithium disilicate was the major phase. The LD proved to be strong (3p-bending strength of 233 ± 12 MPa) and bioactive after 14 days of immersion in SBF. In terms of lithium ion release, the LD was outside the toxic range (> 8.3 ppm). The LM and LD are not cytotoxic. The LD shows the best cellular adhesion and proliferation, leading to the formation of a mineralized matrix after 21 days. These results clearly suggest that the new LD brand is strong and highly biocompatible and warrants further study.

1. Introduction

Many bioactive glasses, including the pioneer Bioglass 45S5, have been extensively studied since the early 70s and are being used as bone regenerative materials in orthopedic and dental applications [1,2]. However, for treating large bone defects or replacing small bones, good fracture strength (> 300 MPa) and toughness (> 2.5 MPa·$m^{1/2}$) are essential [3]. Due to the interconnected microstructure, and consequently, high strength [4,5], glass-ceramics based on lithium disilicate have been used in dentistry for > 15 years, despite their inertness. The possibility of developing a bioactive glass-ceramic containing lithium meta or disilicate crystals has aroused great interest in bone reconstruction [6]. As preliminary result, the fracture toughness of our new material (> 200 MPa) can be compared with that of Bioglass 45S5 (40–60 MPa) [3].

Notwithstanding, a concern regarding this new material is that lithium may be both beneficial and harmful, depending on its concentration in the blood plasma. Studies [7,8] suggest that the Li therapeutic range in plasma is up to 8.3 μg/mL, and the acceptable range is up to 17.3 μg/mL. At concentrations above 20 μg/mL, there is a risk of death. Lithium is used as an active drug in many compositions [9–12] and because of that, studies of its releasing should be very carefully carried out. Moreover, other studies have demonstrated the action of Li at cellular level, such as increased proliferation of cells and osteogenic and cementogenic differentiation [13,14].

In an attempt to ally Li^+ actions at the cellular level with the regenerative properties of Bioglass 45S5, some studies have investigated the replacement of certain oxides from the original composition of Bioglass 45S5 by Li_2O. For instance, Khorami et al. [15] evaluated the bioactivity and biocompatibility of Bioglass 45S5 with different concentrations of Li_2O as substitutes for Na_2O. The composition with the highest degree of substitution (12 mol% Li_2O) showed high bioactivity.

* Corresponding author.
E-mail address: ju_daguano@yahoo.com.br (J.K.M.B. Daguano).

https://doi.org/10.1016/j.msec.2018.09.006
Received 18 October 2017; Received in revised form 5 August 2018; Accepted 3 September 2018
Available online 05 September 2018

Furthermore, the rate of cell proliferation and osteogenic differentiation were increased, showing the efficiency of this ion as a bone stimulator. However, intermediate compositions (with 3% and 7 mol% Li_2O) were not able to form hydroxyl carbonate apatite (HCA) crystals in SBF up to 21 days demonstrating that the relationship between HCA formation and the amount of lithium in the sample is strongly dose-dependent. Miguez-Pacheco et al. [8] showed that the addition of lithium did not prevent the formation of an HCA layer on the surface of scaffolds. However, the composition with the highest Li_2O degree of substitution (10 wt%) perhaps could exceed the concentration considered therapeutic (< 8.3 μg/mL Li^+ in the blood), indicating a need for attention with glass formulation.

The proposal of our work was not to study the incorporation of lithium in a known bioactive glass, but to develop a brand-new glass-ceramic based on the Li_2O-SiO_2 system with a residual bioactive glass. To the best of our knowledge, this is the first study ever to develop a lithia-silica bioactive glass-ceramic. In multicomponent glasses, the formation of crystalline phases after appropriate thermal treatment is much more complex than in the simple binary Li_2O-SiO_2 system [16,17]. In multicomponent glasses, crystallization typically occurs in two stages: first, the formation of a lithium metasilicate phase (Li_2SiO_3), and then, as the temperature increases, this phase transforms into lithium disilicate ($Li_2Si_2O_5$) [18,19]. Lithium metasilicate glass-ceramic is an intermediate material used in computer-aided-manufacturing (CAD/CAM) processes for all ceramic lithium disilicate glass-ceramic restorations [20,21]. Thus, in this work, we studied samples containing both lithium metasilicate and lithium disilicate crystal phases.

The overall objective of the present study thus to develop and elucidate the *in vitro* biocompatibility of new LS glass-ceramic materials, by lithium release, bioactivity, cytotoxicity, cell adhesion and proliferation, as a fundamental step aiming at the application of the new material for bone restoration.

2. Materials and methods

2.1. Glass synthesis

The nominal glass composition is shown in Table 1. This composition corresponds to a nominal mixture of 80 mol% lithium disilicate ($Li_2O{\cdot}2SiO_2$) and 20 mol% of a (bioactive) residual glassy matrix with a density similar to that of the crystal phase ($Li_2O{\cdot}2SiO_2$). A home-made, proprietary software, Reformix 3.0 was used for that purpose. Lithium carbonate (99%, Synth, Brazil), high-purity quartz powder (SiO_2 – Vitrovita, Brazil), calcium carbonate (98%, J. T. Baker, USA), potassium carbonate (99%, Sigma-Aldrich, Germany), phosphorus pentoxide (99%, Vetec, Brazil), strontium carbonate (97%, Vetec, Brazil), zinc oxide (99.7%, J.T. Baker, USA) were used. The as-received powders were weighed and mixed to obtain the desired formulation 64.3% SiO_2-26.7% LiO_2-4.4% K_2O-2.0% CaO-1.8% P_2O_5-0.6% SrO-0.2% ZnO. The mixed reagents were then fused in a platinum crucible at about 1450 °C, cast and remelted three times to promote homogenization, and, finally, cast onto a disk-shaped mold and annealed at a temperature 60 °C below the glass transition, T_g, for 2 h.

2.2. Glass-ceramic preparation

A differential scanning calorimetry (DSC) run was carried out to estimate the crystallization temperature peaks of the parent glass. A monolithic glass sample was heated from room temperature to 1000 °C, with a heating rate of 15 °C/min. The experiment was performed in a NETZSCH DSC404 F1 thermal analyzer using platinum crucibles under air atmosphere.

Based on the DSC results, different heat treatments were performed in a horizontal electric furnace with the temperature controlled to within ± 1 °C, to obtain glass-ceramics of the desired composition. The furnace heating rate was 10 °C/min.

2.3. Microstructural analysis

We used XRD to investigate the development of crystalline phases upon heat treatment. Disks of 12 mm diameter and 2 mm thick were prepared and XRD data were collected on a diffractometer (Bruker AXS, D8 Focus) using CuKα radiation. The samples were scanned to cover diffraction angles, 2θ, from 10° to 60°, with a step size of 0.02° and a collection time of 2 s. The crystalline phases were identified using the Joint Committee for Powder Diffraction Studies (JCPDS) standard diffraction patterns. The amount of crystal phases (crystallized volume fraction) was estimated according to the procedure used by Daguano et al. [22] The Crystallinity Index, CI %, was calculated from the diffractogram of each glass-ceramic. For evaluating the crystalline area, A_C, and the total area, A_T (A_T = amorphous + crystalline), the following equation was used:

$$CI\% = (A_C/A_T) \times 100\%$$

Data management and analysis were performed using Origin® 8.5 software. To analyze the microstructure, the samples were polished (with 1200-grit SiC paper and a 1 μm diamond suspension) and subsequently etched using H_3PO_4 37%. After the chemical etching, the samples were sputtered with Au for SEM analysis. Images were produced by scanning electron microscopy (Quanta 250 SEM-FEI).

2.4. Mechanical characterization

The flexural strength (σ_f) was measured for six cylinders of Φ12 × 35 mm of the LD glass-ceramic. A three-point bending setup (Instron Universal Test Machine Model 4202) at a crosshead speed of 0.2 mm/min was used. No surface finish was applied to the samples. This test was performed according to the ASTM C158-84 standard [23].

2.5. In vitro bioactivity test

To evaluate the bioactivity of the synthesized materials, *in vitro* tests were performed according to the method described by Kokubo and Takadama [24]. The simulated body fluid (SBF) used in this study was acellular and protein-free with a pH of 7.25. The volume of SBF used in the bioactivity tests is related to the surface area of the sample. According to the procedures described by ISO 23317-07 [25], for a dense material, the appropriate volume of solution should obey the following relationship:

$$Sa/Vs = 0.1\ cm^{-1}$$

where *Vs* represents the volume of SBF (mL) and Sa represents the total geometric surface area of the sample (mm^2).

For this test, the glass and glass-ceramic cylinders were cut into 12 mm diameter/2 mm thick discs using a diamond-blade. Finally, the discs were ground using silicon carbide paper to a grit of 400 (~35 μm)

Table 1
Batch composition of the intended (designed) glass-ceramic.

Fraction	(mol%)	Oxide (mol%)					
Crystalline	80%	66.6% SiO_2			33.3% Li_2O		
Amorphous	20%	55% SiO_2	22% K_2O	10% CaO	9% P_2O_5	3% SrO	1% ZnO

and cleaned with acetone in an ultrasonic cleaner for 2 min. After drying, they were immersed during 1, 3, 7, 14 and 21 days in SBF solution in sterilized polypropylene flasks at 37 °C. The test was made in triplicate and SBF solution was refreshed every 3 days.

Chemical groups on the surface of the samples were identified by Fourier Transform Infrared Spectroscopy (FTIR) in diffuse reflectance mode. The IR spectra were measured in the range of 4000–400 cm^{-1} at a resolution of 4 cm^{-1} using VARIAN 660-IR spectrometer.

After the soaking times, selected samples were evaluated by XRD and SEM.

2.6. Degradation tests

Samples of glass and glass-ceramics ($n = 10$) were weighed and their surface areas were calculated. Then, they were immersed in Tris-HCl solution (pH 7.4, 37 °C) at ratio 0.1 cm^{-1} (surface area/solution volume). The solution was replaced twice a week. The samples were taken out after 1, 3, 7, 14, 21 and 28 days, rinsed off with deionized water, dried and weighed again. The weight loss (W_L) was calculated as follows:

$$W_L = (W_0 - W_d)/W_0 \times 100\%$$

where W_0 denotes the initial weight of the samples, and W_d represents the weight of the dried samples after the scheduled immersion time.

In order to evaluate the amount of lithium release, samples of each group were placed individually into sterilized polypropylene flasks. The flasks were filled with Tris-HCL solution (pH 7.4) and maintained at 37 °C during 1, 3, 7, 14, 21 and 28 days. After each period of immersion, the ionic concentration of lithium in Tris-HCl solutions was measured by Flame Atomic Absorption Spectrometer (Varian, Spectr-AAS-220-FS). The measurements were made in triplicate.

2.7. In vitro cytotoxicity test

The Balb/c cells were employed for cytotoxicity analysis. Cells were maintained on a regular feeding regime in a cell culture incubator at 37 °C/5% CO_2/95% air atmosphere. Cells were seeded into 96 well plates at a density of 2×10^4 cells per well and incubated for 24 h prior to testing with liquid extracts. The culture media used was DMEM supplemented with 10% fetal bovine serum. The samples were immersed in the cellular medium at final concentration of 6 cm^2/mL during 3 days under gently shaking. After this time, we extracted the samples. The cell viability samples were evaluated using the Methyl Tetrazolium (MTS) assay in 96 well plates. Liquid extracts were added into wells containing Balb/c cells in culture medium. The prepared plates were incubated for 24 h at 37 °C/5% CO_2. The MTS assay was then added and the cultures were reincubated for further 2 h (37 °C/5% CO_2). Next, the cultures were removed from the incubator and the absorbance was measured at a wavelength of 490 nm. A sterile medium was used as a control, and the cells were assumed to have metabolic activities of 100% in normal medium culture. The cell viability was calculated as follows:

$$\textit{Cell viability} = (OD_{sample}/OD_{control}) \times 100\%,$$

where OD_{sample} = optical density of the sample and $OD_{control}$ = optical density of the control.

2.8. Cell adhesion and proliferation

MG63 cells (human osteosarcoma) were cultured in Minimum Essential Medium (MEM) supplemented with 10% fetal bovine serum in a cell culture incubator at 37 °C/5%CO_2/95% air atmosphere. The glass and glass-ceramic discs were briefly ground in water with silicon carbide paper 400 grit, cleaned with acetone and sterilized prior to cell culture.

The cells were seeded onto the disc sample surfaces in 24-well polystyrene plates at a density of 2×10^4 cells/well and incubated at 37 °C in a humidified atmosphere with 5% CO_2. After 1, 3, 7, 14 and 21 days. At each day, one sample with the MG63 cells growing was used to evaluate the viable cell MTS reaction, which product of the reaction is water soluble. The samples were taken from the original wells and placed in new ones, the proportion of (cell medium) / (MTS solution) was kept according to the manufacturer's instructions (Promega). After the standardized incubation time with the MTS and color developed, the sample medium was read in an ELISA reader (Thermo – Multiskan EX). Other batches of the films were washed 2 times with PBS 1× and fixed with 4% (v/v) formaldehyde in 0.9% (w/v) sodium chloride solution for 30 min and, dehydrated in a graded series of alcohol, and stained with 2% Alizarin red (pH 4.2). Finally, they were photographed using a confocal laser microscope (Olympus LEXT OLS4100).

2.9. Statistical analysis

Statistical data analyses were conducted using a one-way analysis of variance (ANOVA) and Student's *t*-test. The level of significance was 0.05.

3. Results

A DSC curve of the base glass is shown in Fig. 1. The glass transition temperature (T_g) is approximately 450 °C. The two well-defined exothermic peaks (640 °C and 772 °C) are characteristic of lithium metasilicate (LM) and lithium disilicate (LD) crystal phases, respectively. In addition, the small exothermic peak at 733 °C corresponds to lithium phosphate (LP) crystallization, as we will discuss below.

The DSC data was used to design the nucleation and the crystallization schedules of the glass to obtain two types of glass-ceramics (LM – lithium metasilicate and LD – lithium disilicate, as major phases) in double-stage heat treatment processes. Samples were further treated at different temperatures, in accordance with Table 2, and also cooled down at a rate of 3 °C/min in order to induce the desired crystallization of the glass.

Fig. 2 shows the crystalline phases identified by XRD and the value of the crystallinity index (CI %), for each sample. XRD pattern of the glass sample (Fig. 2a) did not display any diffraction peaks, confirming the amorphous state of the sample. For the LM sample (Fig. 2b), lithium metasilicate (Li_2SiO_3) was detected as the major phase. A single peak could be observed at approximately $2\theta = 27°$ which indicated the formation of the lithium phosphate (Li_3PO_4) as a crystal phase. Finally, XRD pattern of the LD sample (Fig. 2c) showed lithium disilicate ($Li_2Si_2O_5$) as the principal phase coexisting with Li_3PO_4 as a minor phase. The LM sample had approximately 42% of crystallinity, whereas the remaining matrix was still amorphous. The degree of crystallinity

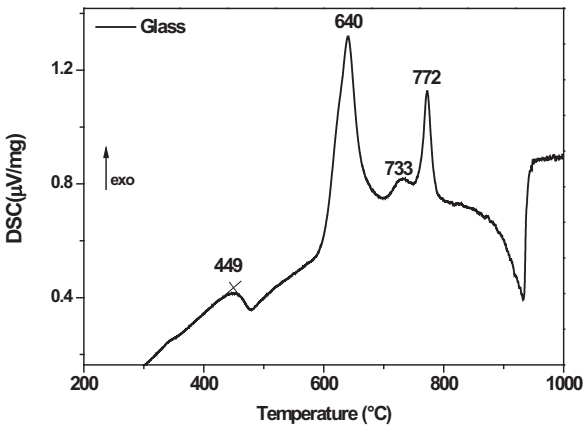

Fig. 1. DSC curve of parent glass.

Table 2
Designation of samples obtained by double-stage heat treatment.

Samples	Nucleation		Growth	
	Temperature (°C)	Time (min)	Temperature (°C)	Time (min)
Glass	–	–	–	–
LM	504	60	670	90
LD	504	60	777	360

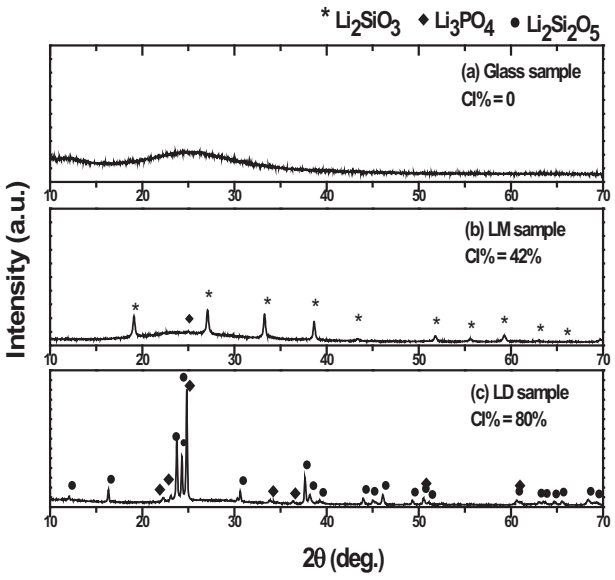

Fig. 2. XRD pattern of samples (a) glass, (b) LM, (c) LD. Crystal phases are identified, and the index of crystallinity, CI %, is also indicated.

(CI %) increased considerably to about 80% (as predicted in our original formulation) in the LD sample.

Fig. 3 shows Scanning Electron Microscopy micrographs of the glass-ceramics after chemical etching. The lithium metasilicate microstructure is perceptible in Fig. 3(a), whereas Fig. 3(b) shows lithium disilicate crystals embedded in a glassy matrix. A large number of rod-like lithium disilicate crystals are evident and their orientations are random, creating an interlocking microstructure.

Table 3 shows the bending strength (σ_f) results obtained for the LD glass-ceramic and values of some commercial materials.

The average bending strength of our best material, LD glass-ceramic (233 MPa), is significantly greater than that of Bioglass 45S5® (the pioneer bioactive material), and comparable to that of IPS e.max® CAD (commercial lithium disilicate glass-ceramic), with the great advantage that of being much more bioactive.

Table 3
Values of bending strength of several materials [26,27,28].

Dental materials	Bending strength (MPa)	Bioactive materials	Bending strength (MPa)
LD glass-ceramic	233 ± 12	Bioglass 45S5®	40–60
IPS e.max® CAD	262–360	Cerabone® A-W	220
IPS Empress	120–180	Ceravital®	100–150

Figs. 4-6 illustrated the apatite-mineralization ability of glass, LM glass-ceramic and LD glass-ceramic, respectively.

After immersion in SBF for 3 weeks, the FTIR spectra (Fig. 4a) suggested that there was no significant change in the composition of the material. Only bands at ~470 cm^{-1} and 1090 cm^{-1} could be observed and were attributed to the Si—O—Si bond. After the first day of immersion, a band could be seen in the region of 1250 cm^{-1} which was also related to the vitreous structure [11].This was confirmed by the XRD patterns (Fig. 4b), characterized by a broad halo centered at ~25° (2θ), which is a typical feature of silicate glasses. Fig. 4(c) shows surface morphologies of the glass samples after 14 and 21 days of soaking in SBF solution. The surface appearances for all the samples after immersion were relatively rough, indicating a leaching process on the glass surfaces after immersion in SBF.

For the LM glass-ceramic, as well as the parent glass, the bonds found in the spectra result from silicate and phosphate groups from the intrinsic structure of the material. Thus, characteristic peaks of HCA were also not observed. From XRD, two crystalline phases were identified (lithium metasilicate PDF #72–1140: Li_2SiO_3 and lithium phosphate PDF 15–760: Li_3PO_4), hence there was no transformation or formation of new phases during the bioactivity test. The micrographs show alterations on the sample surface, *i.e.* it is possible observe the leaching effect of the SBF. However, the FTIR and XRD analyses did not show the formation of an HCA layer on the sample surface.

Before immersion in SBF, the spectrum presents the original chemical bonds from the intrinsic material structure [19,29], Fig. 6(a). After 14 days, the material already presented other bands characteristic of bioactive materials, indicating that the process of formation of the HCA layer began within this time interval. The presence of calcium-phosphate deposition on the surface of the samples, such as HCA, was also observed by phosphate bands at 605 and 565 cm^{-1} (P—O bending) [30]. These bands became more defined with increased reaction time. Although there are characteristic peaks of HCA, after 14 days of

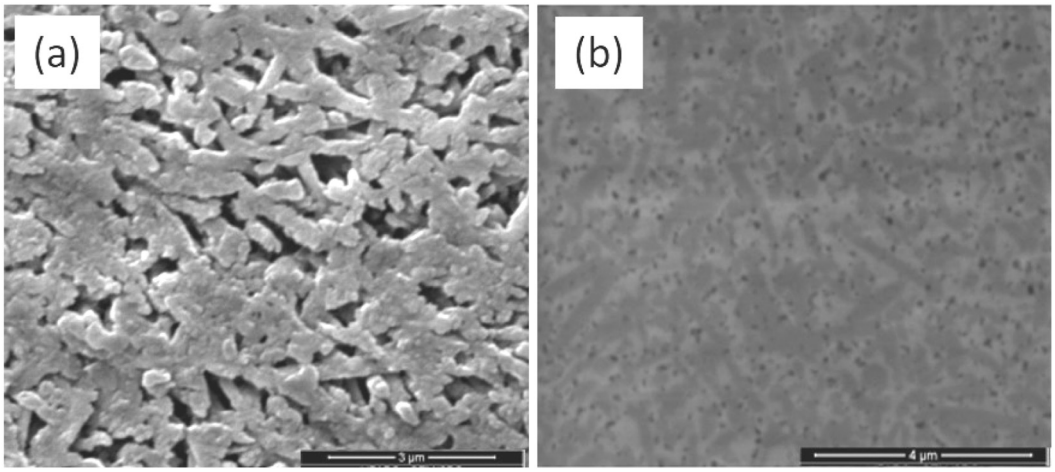

Fig. 3. SEM micrographs of (a) LM glass-ceramic and (b) LD glass-ceramic.

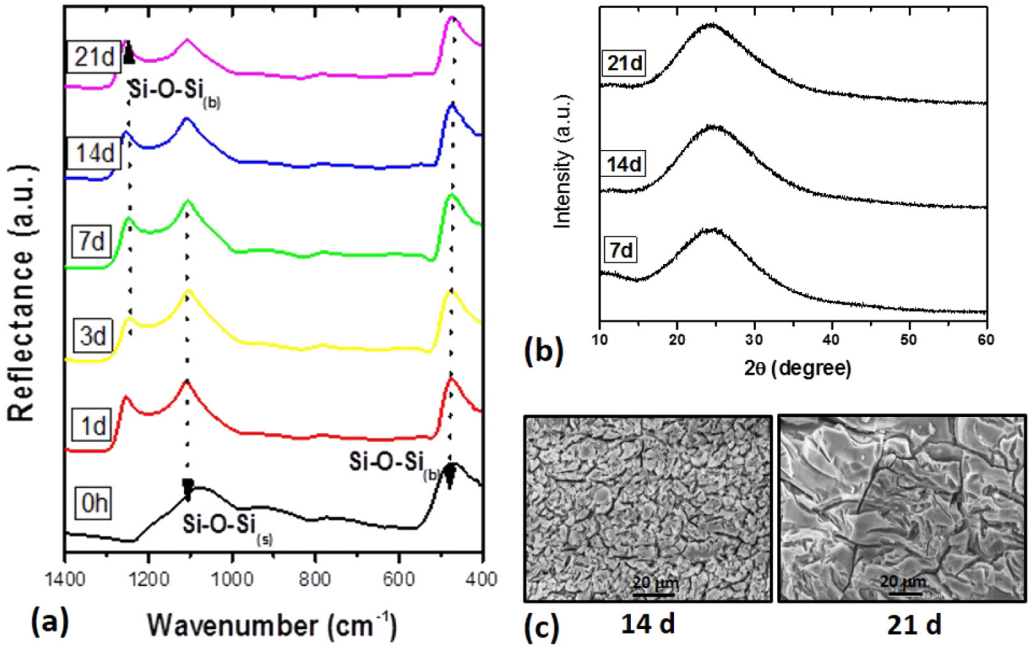

Fig. 4. Apatite-mineralization ability of glass samples (a) FTIR spectra before (unreacted – 0 h) and after (1, 3, 7, 14, 21 days) *in vitro* bioactivity tests, (b) XRD patterns after (7, 14, 21 days) immersion in SBF, and (c) SEM micrographs after (14, 21 days) immersion in SBF.

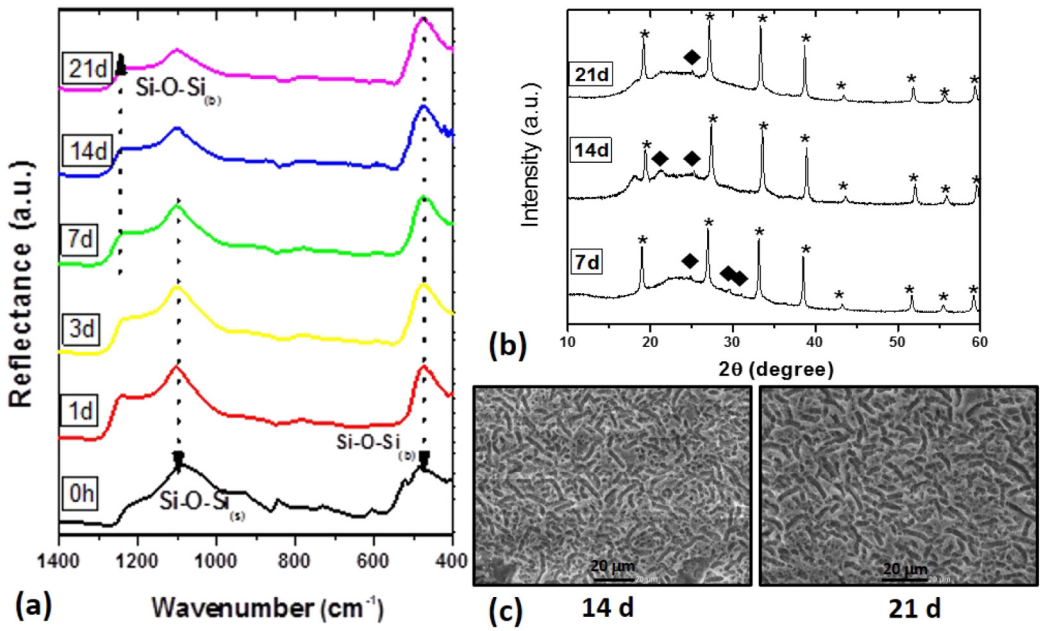

Fig. 5. Apatite-mineralization ability of LM glass-ceramics (a) FTIR spectra before (unreacted – 0 h) and after (1, 3, 7, 14, 21 days) *in vitro* bioactivity test, (b) XRD patterns after (7, 14, 21 days) immersion in SBF (* PDF 72–1140: Li_2SiO_3, ♦ PDF 15–760: Li_3PO_4), and (c) SEM micrographs after (14, 21 days) immersion in SBF.

exposure to SBF, there is still a band in the region around to 470 cm^{-1}. This band, that was also present in the spectra after smaller immersion times, was related to the Si—O bonds in the material. This indicated the possibility that not all the surface of the material had been covered by HCA. Characteristic bands of carbonates (CO_3^{2-}) were detected at 1410 cm^{-1}, but it was only possible to observe the presence of CO_3^{2-} after immersion of the samples in SBF for 21 days (not pronounced bands). Such evidence is consistent with the absence of calcite on the surface of these samples, as observed in the XRD patterns.

XRD analysis was performed to characterize the precipitates and a diffractogram is illustrated in Fig. 6(b). The XRD patterns of the samples after 14-day immersion in SBF exhibited a broad peak centered at ~32° (2θ). This peak may be attributed to the presence of hydroxyapatite (HA), but the intensity of which is not sufficiently strong to establish the feature of this phase. XRD patterns obtained for the glasses after 21 days in contact with SBF showed two peaks at approximately 26 and 32° (2θ), corresponding to the HCA-like phase. After soaking in SBF solution, the surface morphologies showed the presence of a precipitate layer with crevices on the surface of the samples, as illustrated in Fig. 6(c). The formation of cracks is likely due to the shrinkage of the precipitate during the drying process. However, the surface showed relatively smaller cracks, implying a thinner precipitate layer.

The FTIR, XRD and SEM results show evidence of bioactivity of the LD glass-ceramic by the formation of an apatite layer on the surface, indicating its apatite-mineralization capability in SBF solution.

The dissolution rates of the glass and glass-ceramics as function of

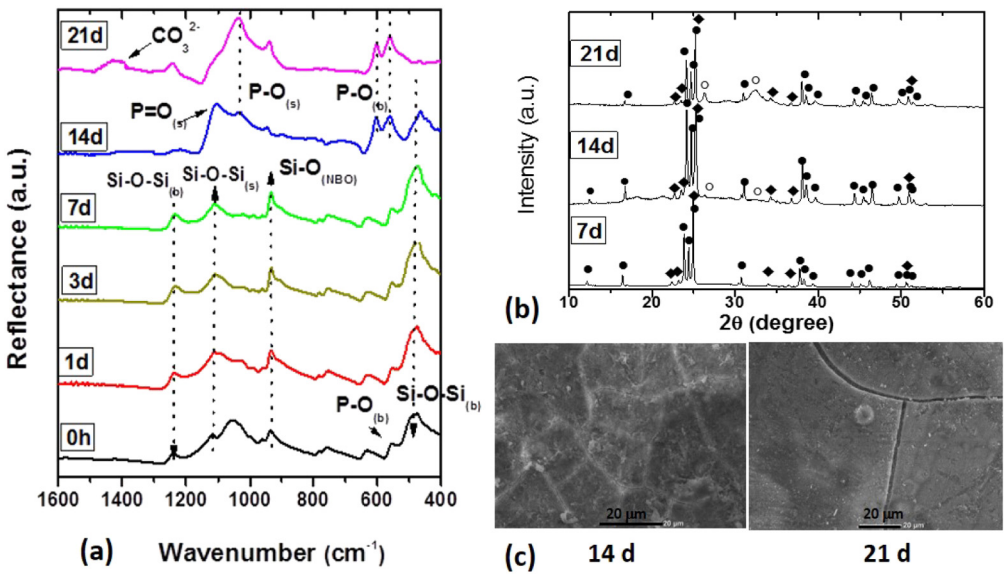

Fig. 6. Apatite-mineralization ability of LD glass-ceramics: (a) FTIR spectra before (unreacted – 0 h) and after (1, 3, 7, 14, 21 days) *in vitro* bioactivity test, (b) XRD patterns after (7, 14, 21 days) immersion in SBF (● PDF 72–102: $Li_2Si_2O_5$, ♦ PDF 15–760: Li_3PO_4, ○ PDF 19–272:$Ca_{10}(PO_4)_3(CO_3)_3(OH)_2$), and (c) SEM micrographs after (14, 21 days) immersion in SBF.

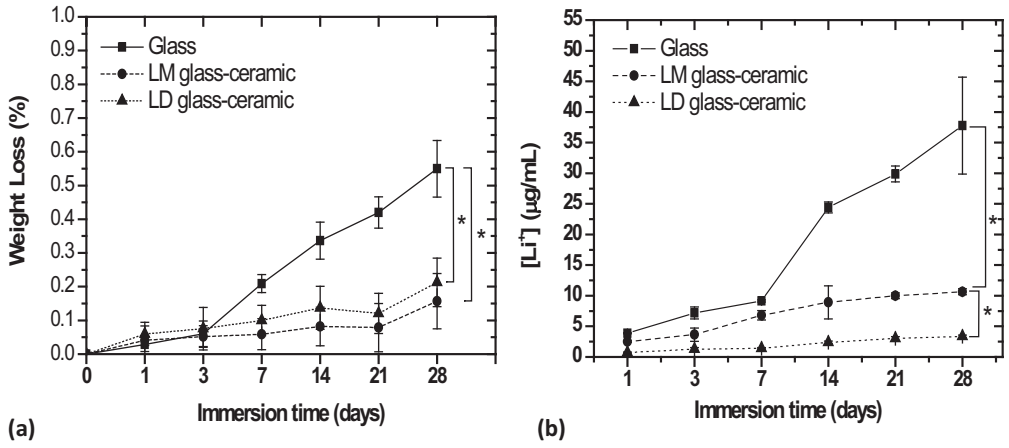

Fig. 7. Dissolution ability of glass, LM and LD glass-ceramic samples in Tris-HCl solution (a) Weight losses as function of immersion time. (b) Ionic concentration of Li after 1, 3, 7, 14, 21 and 28 days of soaking (*denotes significant statistical difference between two groups: $p < 0.05$).

immersion time are shown in Fig. 7.

Fig. 7(a) shows that the weight loss after 3 days of immersion in Tris-HCl solution were 0.06 ± 0.04%, 0.05 ± 0.03% and 0.08 ± 0.06% for the glass, LM glass-ceramic and LD glass-ceramic, respectively. After this time, an initial increase was observed in weight loss for the glass samples and reached 0.55 ± 0.08% for 28 days of immersion. At the same time point, the LM and LD glass-ceramics showed 0.16 ± 0.08% and 0.21 ± 0.07% of weight loss, respectively.

The lithium release profile is shown in Fig. 7(b). For the three groups, lithium release increased with immersion time. Until 7 days of immersion, the glass and glass-ceramics presented Li^+ levels in the solution within the accepted ranges for humans (≤17,4 μg/mL) [31]. After this period, the concentration of lithium released for the glass ranged from 9.2 ± 0.2 μg/mL to 38 ± 8 μg/mL over 7–28 days. In the case of the LM glass-ceramic, the lithium concentration in the solution was equal to 10.6 ± 0.5 μg/mL after 28 days of immersion. For the LD glass-ceramic, the Li^+ levels remained relatively constant, ranging from 1.4 ± 0.1 μg/mL to 3.4 ± 0.2 μg/mL over 7–28 days.

In vitro cytotoxicity analysis by the MTS metabolic activity assay is shown in Fig. 8. This assay revealed that the glass and the glass-ceramics were non-cytotoxic, with cell viability up to 70%. According to the ISO 10993-5 [32], a material is considered cytotoxic when it decreases 30% cell viability [33]. There is significant statistical difference between all groups analyzed.

The cell adhesion and proliferation statistics for all samples are shown in Fig. 9. Table 4 confirms the viability of the cells growing on the surface of the glass-ceramics. Over 21 days of MG-63 cells culture, ‘q cell attachment could be observed on the glass sample surface (Fig. 9(a)). For the LM glass-ceramic, as shown in Fig. 9(b), osteoblast-

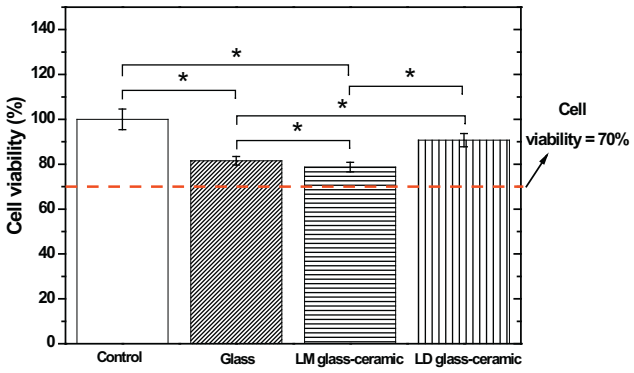

Fig. 8. Cell viability of the control, Glass, LM glass-ceramic and LD glass-ceramic extract.

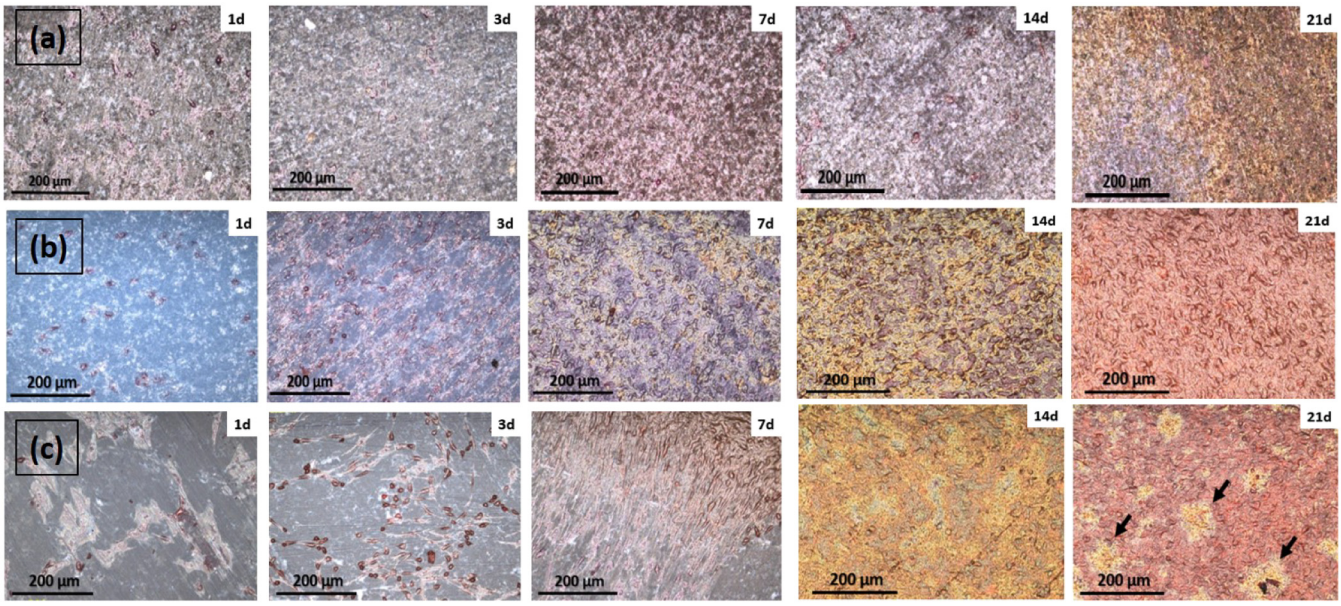

Fig. 9. Cell adhesion and proliferation up to 21 days for (a) glass, (b) LM glass-ceramic and (c) LD glass-ceramic. Arrow: osteogenic differentiation evidenced by calcified matrix stained with Alizarin Red.

Table 4
Optical density measured at wavelength 490 nm of the MTS reacted with the MG63 cell on the samples.

Samples	Days				
	1	3	7	14	21
Glass	0.240	0.348	0.410	1.019	0.940
LM glass-ceramic	0.112	0.261	0.423	0.852	0.954
LD glass-ceramic	0.023	0.276	0.527	0.852	1.280

like MG-63 cells cultured on the samples showed increasing proliferation throughout the time of analysis. Finally, about LD glass-ceramic, the results of cell adhesion and proliferation test are also presented in Fig. 9(c). The MG63 viability is also confirmed by MTS (Table 4). After 14 days cell seeding, MG-63 cells were attached and proliferated on almost the entire surface of the sample. At day 21, some random yellowish/brownish areas of calcified matrix could be observed.

4. Discussion

The findings of DSC and XRD studies were consistent with those in multicomponent lithia-silica glasses. For instance, Zhang et al. [19] verified the presence of two crystallization peaks, the first at 645 °C and the other at 827 °C, which correspond to the formation of lithium metasilicate and lithium disilicate, respectively. Soares et al. [18] also found two crystallization peaks in two different compositions of multicomponent glasses, one for the metasilicate and another for the lithium disilicate. However, only in the composition with higher silica content, the total conversion of the metasilicate to disilicate was observed after heat treatment. The other composition showed the existence of both metasilicate and lithium disilicate phases. Therefore, our XRD results indicated that the chosen treatments were effective in obtaining the desired crystalline phases.

The mechanical properties of these lithium disilicate glass-ceramics depend on various factors, especially their microstructure. In general, the high mechanical strength of these glass-ceramics ($\sigma_f > 200$ MPa, $K_{IC} > 2$ MPa·m$^{1/2}$) [27] is due to their interlocked microstructure with high crystallinity (above 60%) [34], and small (0.5–3 µm) [35] crystals of high aspect ratio, which promote crack bridging and deflection, and hinder crack propagation [5,27]. In our study, the LD glass-ceramic also shows an interlocking microstructure, crystals with high aspect ratio, size near 2 µm, and high crystallinity (around 80%). Thereupon, as a preliminary result, our LD also demonstrates a high fracture strength.

The most striking result from the bioactivity study was that only the LD glass-ceramic was bioactive. It is known that, for the HCA layer to form on the surface of a material, its dissolution rate and the apatite precipitation rate must be compatible [24,36,37]. In order to yield apatite quickly, a bioactive glass obtained by cast processing must present a medium percentage of SiO_2 (typically between 44 and 50 mol %) [38]. During a bioactivity test, when the quantity of Si is too low, the initial amorphous silicate network is more depolymerized, and the reaction requires a longer time to obtain, as according Hench's mechanism [39,40], a highly polymerized silica gel phase on which the amorphous calcium phosphate will precipitate. If the Si rate is too high, the highly polymerized network slows down the migration of phosphate groups and delays the formation of HCA at the surface. These results are in agreement with our results, which showed no bioactivity for the glass and the LM glass-ceramic. This result was expected because the parent glass had 64.3 mol% SiO_2, whereas the LD glass-ceramic had 55 mol% SiO_2 in the residual glass. Also, for glass-ceramics, the silica content in residual glass is strongly correlated with crystallinity and composition, which jointly influence material's the bioactivity.

The chemical durability of glass-ceramics also depends on the composition of the residual glass [41,42]. Although some mass loss of samples occurred, the quantities were very low, not exceeding 1%. This finding corroborated the ideas of He et al. [43], who suggested a mass loss for β-TCP of 0.3 ± 0.1%, after 7 days of immersion in Tris-HCl solution, reaching 1.0 ± 0.2% after 28 days. Also, a hydroxyapatite ceramic presented a more stable behavior, exhibiting a loss of mass of only 0.05 ± 0.02% during the analyzed period of time, resembling the behavior observed for the LM and LD glass-ceramics.

A correlation was found between weight loss and lithium release profile. The glass presented higher degradation rates, probably due to the greater capacity of dissolution in aqueous medium. As the material is amorphous, its ions are more available to establish ionic exchanges [37]. In aqueous media, the Li^+ ions are replaced in the glass network by H^+, allowing the formation of Si—OH groups. This phenomenon explains the high concentrations of lithium in the analyzed solutions.

The exchange reaction between the lithium-based glass and the aqueous medium can be represented by the equation [42]:

$$Glass{\equiv}Si{\blacksquare}O{\blacksquare}Li + H^{+} \leftrightarrow Glass \equiv Si{\blacksquare}O{\blacksquare}H + Li^{+}$$

For the LM sample, the highest release of Li^{+} occurred in 28 days of immersion ($[Li^{+}] = 10.6\,\mu g/mL$). Although relatively high, this Li^{+} concentration is in the acceptable range. There was a marked difference between the glass and LM samples. LM sample presented a higher stability and a lower rate of dissolution with the medium, due to the crystalline fraction of the material, where part of Li^{+} ions is trapped. However, a considerable amount of lithium can still be released into the medium. According to XRD results, a considerable amorphous fraction is still present, providing ion exchange with the solution.

For the LD sample, the concentration of Li^{+} remained within the range considered therapeutic throughout the immersion period ($[Li^{+}] = 3.4\,\mu g/mL$ for 28 days). This material showed CI near 80%, which indicates that almost all lithium of the composition is trapped in the crystalline phase, with a few free Li^{+} ions remaining to promote exchanges with the medium. In this case, only the residual vitreous phase is available for exchange. This result corroborated the results of bioactivity.

From the data of Fig. 7(b) is possible to establish linear equations from the time × lithium release. For the glass, LM and LD glass-ceramics, the linear trend equations obtained were, respectively:

$$y_{glass} = 1.33x + 1.96 \quad R^2 = 0.98$$

$$y_{LM} = 0.35x + 2.37 \quad R^2 = 0.85$$

$$y_{LD} = 0.11x + 0.59 \quad R^2 = 0.93$$

where x represents the time in days and y represents $[Li^{+}]$ in the medium. Thus, such equations are useful to predict the lithium concentrations for longer times, assuming that the release profile remains the same.

Regarding the *in vitro* cytocompatibility, although all materials were non-cytotoxic, each of the materials promoted a different cellular stimulus. In all samples are observed cell attached and their proliferation rate varies according to the materials phases. In the first day, glass seems to favor the cell attachment, but the growth stimulus is better observed on the LD sample. At 14 and 21 days of cell contact, there is evidence of the process of matrix mineralization, especially after 21 days, where the surface of LD samples is more covered and HCA nucleation is observed. These results showed the behavior of a material with characteristics to generate foreign body reactions after implantation in the organism. On the other hand, lithium metasilicate promoted cell adhesion and proliferation. Initially, after 1 and 3 days, individualized cells adhering to the material could be noticed (cells stained in red). At 7 days, good confluence of the cells was observed, as there were cells all over the surface, indicating cell proliferation. And after 21 days, the surface of the material was completely filled by cells, forming overlapping cell layers, however with no evidence of the process of matrix mineralization *in vitro*. Thus, the LM samples presented characteristics of a biocompatible material, but osseoconductive behavior instead of osseoinductive as would be desired. Although no major differences between the glass and LM samples had been observed during the growth and differentiation phases of osteogenic cultures, the LD glass-ceramic supported a significant enhancement of calcified tissue areas.

Bone is a type of connective tissue composed of three cell types (osteoblasts, osteocytes and osteoclasts) and a mineralized extracellular matrix [44]. Osteoprogenitor cells only produce a bone-like matrix in favorable environments, where they can adhere and proliferate, since it is no longer possible to grow, they begin to secrete mineralized matrix forming nodules of calcification [45]. In this way, in 21 days, calcification nodules could be identified in micrographs (black arrows). This study confirmed that the LD glass-ceramic surface is an environment suitable for cellular development, which is fundamental for establishing a satisfactory implant-tissue interaction [46].

A strong relationship between biological properties and composition of different bioactive glasses has been reported in the literature. Certain ions improve their interactivity with cells. Sr^{2+} and Zn^{2+}, for example, influence the bioactivity of the material, stimulating osteoblastic and osteoclastic activity [46–49]. Regarding lithium, it is known that it has numerous protective effects in cell media, as well as some harmful effects, being dose-dependent [31,50]. We have used all this information in the design of this brand-new lithia-silica glass-ceramic. Former results with (non-bioactive) glass-ceramics of the same family and its microstructure indicates that it may show optimum mechanical properties, which must still be evaluated. We are also performing *in vivo* studies.

5. Conclusions

We designed and produced a novel lithium silicate glass-ceramic, with about 80 vol% of lithium disilicate crystals, bending strength of 233 MPa and evaluated their *in vitro* biocompatibility. The most significant finding was that, unlike the parent glass and other existing glass-ceramics of the same family, this new lithia-silica glass-ceramic is bioactive! It promoted cell adhesion and proliferation, and induced the MG-63 cells to produce a bone-like matrix. Hence, this study made several noteworthy contributions to the development of a new biomaterial with potentially good fracture strength, which may be quite relevant for bone regeneration in orthopedic and dental applications.

Acknowledgments

This work was supported by the Multiusers Central Facilities of UFABC and Laboratory of Biomaterials and Biomedical Devices of UFABC. J. Daguano would like to thank CNPq (Grant n°. 430057/2016-4). A. Rodas would like to thank FINEP (grant nº 04.13.0481.01) and FAPESP grant num. 2015/02265-7 and Dr. Olga Higa for allowing us to use the cell culture facilities at IPEN/CNEN-SP. EDZ is grateful to the São Paulo Research Foundation - Fapesp – for generous funding, grant number 2013/00793-6. This study was financed in part by the Coordenação de Aperfeiçoamento de Pessoal de Nível Superior - Brasil (CAPES) - Finance Code 001. Also, J. Daguano is grateful to Wanderlei S. Santos and Wilson Souza for providing mechanical test help.

References

[1] L.L. Hench, Bioceramics: from concept to clinic, J. Am. Ceram. Soc. 74 (1991) 1487–1510.
[2] J.R. Jones, Review of bioactive glass: from Hench to hybrids, Acta Biomater. 9 (2013) 4457–4486.
[3] T. Kokubo, H. Kim, M. Kawashita, Novel bioactive materials with different mechanical properties, Biomaterials 24 (2003) 2161–2175.
[4] E. Apel, J. Deubener, A. Bernard, M. Holand, R. Muller, H. Kappert, V. Rheinberger, W. Holand, Phenomena and mechanisms of crack propagation in glass–ceramics, J. Mech. Behav. Biomed. Mater. 1 (2008) 313–325.
[5] I. Denry, J.A. Holloway, Ceramics for dental applications: a review, Dent. Mater. 3 (2010) 351–368.
[6] M. Montazerian, E.D. Zanotto, Bioactive and inert dental glass-ceramics, J. Biomed. Mater. Res. A 105A (2017) 619–639.
[7] H. Aral, A. Vecchio-Sadus, Toxicity of lithium to humans and the environment — a literature review, Ecotoxicol. Environ. Saf. 70 (2008) 349–356.
[8] V. Miguez-Pacheco, T. Büttner, A.L.B. Maçon, J.R. Jones, T. Fey, D. De Ligny, P. Greil, J. Chevalier, A. Malchere, A.R. Boccaccini, Development and characterization of lithium-releasing silicate bioactive glasses and their scaffolds for bone repair, J. Non-Cryst. Solids 432-A (2016) 65–72.
[9] S.N. Geeva, Lithium entrapped chitosan nanoparticles to reduce toxicity and increase cellular uptake of lithium, Environ. Toxicol. Pharmacol. 61 (2018) 79–86.
[10] S. Bradberry, Lithium, Medicine, 44 2016, pp. 180–181.
[11] A. Moghanian, S. Firoozi, M. Tahriri, Arman Sedghi, A comparative study on the in vitro formation of hydroxyapatite, cytotoxicity and antibacterial activity of 58S bioactive glass substituted by Li and Sr, Mater. Sci. Eng. C 91 (2018) 349–360.
[12] D. Drdlik, M. Slama, H. Hadraba, K. Drdlikova, Jaroslav Cihlar, Physical, mechanical, and biological properties of electrophoretically deposited lithium-doped calcium phosphates, Ceram. Int. 44 (2018) 2884–2891.

[13] P. Han, C. Wu, J. Chang, Y. Xiao, The cementogenic differentiation of periodontal ligament cells via the activation of Wnt/β-catenin signaling pathway by Li^+ ions released from bioactive scaffolds, Biomaterials 33 (2012) 6370–6379.
[14] C. Wu, J. Chang, Multifunctional mesoporous bioactive glasses for effective delivery of therapeutic ions and drug/growth factors, J. Control. Release 193 (2014) 282–295.
[15] M. Khorami, S. Hesaraki, A. Behnamghader, H. Nazarian, S. Shahrabi, In vitro bioactivity and biocompatibility of lithium substituted 45S5 bioglass, Mater. Sci. Eng. C 31 (2011) 1584–1592.
[16] E.D. Zanotto, Metastable phases in lithium disilicate glasses, J. Non-Cryst. Solids 219 (1997) 42–48.
[17] P.C. Soares Jr., E.D. Zanotto, V.M. Fokin, et al., TEM and XRD study of early crystallization of lithium disilicate glasses, J. Non-Cryst. Solids 331 (2003) 217–227.
[18] R.S. Soares, R.C.C. Monteiro, M.M.R.A. Lima, R.J.C. Silva, Crystallization of lithium dissilicate-based multicomponent glasses – effect of sílica/lithia ratio, Ceram. Int. 41 (2015) 317–324.
[19] P. Zhang, X. Li, J. Yang, S. Xu, The crystallization and microstructure evolution of lithium disilicate-based glass-ceramic, J. Non-Cryst. Solids 392–393 (2014) 26–30.
[20] P.C. Guess, R.A. Zavenalli, N.R.F.A. Silva, E.A. Bonfante, P.G. Coelho, V.P. Thompson, Monolithic CAD/CAM lithium disilicate versus veneered Y-TZP crowns: comparison of failure modes and reliability after fatigue, Int. J. Prosthodont. 23 (2010) 434–442.
[21] L. Yin, R. Stoll, Ceramics in restorative dentistry, in: I.M. Low (Ed.), Advances in Ceramic Matrix Composites, Woodhead Publishing Limited, Cambridge, UK, 2014, pp. 624–655.
[22] J.K.M.F. Daguano, K. Strecker, E.C. Ziemath, S.O. Rogero, M.H.V. Fernandes, C. Santos, Effect of partial crystallization on the mechanical properties and cytotoxicity of bioactive glass from the$3CaO{\cdot}P_2O_5$–SiO_2–MgO system, J. Mech. Behav. Biomed. Mater. 14((2012) 78–88.
[23] Astm C158 – 02, Standard Test Methods for Strength of Glass by Flexure (Determination of Modulus of Rupture), (2012), pp. 1–9.
[24] T. Kokubo, H. Takadama, How useful is SBF in predicting in vivo bone bioactivity? Biomaterials 27 (2006) 2907–2915.
[25] ISO DOCUMENT 23317, Implants for Surgery: In Vitro Evaluation for Apatite-forming Ability of Implant Materials, International Organization for Standardization, Geneva, Switzerland, 2007.
[26] A. Willard, T.G. Chu, The science and application of IPS e.Max dental ceramic, Kaohsiung J. Med. Sci. 34 (2018) 238–242.
[27] L. Hallmann, P. Ulmer, M. Kern, Effect of microstructure on the mechanical properties of lithium disilicate glass-ceramics, J. Mech. Behav. Biomed. Mater. 82 (2018) 355–370.
[28] J. Black, G. Hastings, Handbook of Biomaterial Properties, first ed., Chapman & Hall, London, 1998, p. 359.
[29] H.-S. Ryu, J.-K. Lee, J.-H. Seo, H. Kim, K.S. Hong, D.J. Kim, J.H. Lee, D.-H. Lee, B.-S. Chang, C.-K. Lee, S.-S. Chung, Novel bioactive and biodegradable glass-ceramics with high mechanical strength in the $CaO\text{-}SiO_2\text{-}B_2O_3$ system, J. Biomed. Mater. Res. 68 (2004) 79–89.
[30] R.L. Siqueira, N. Maurmann, D. Burguêz, D.P. Pereira, A.N.S. Rastelli, O. Peitl, P. Pranke, E.D. Zanotto, Bioactive gel-glasses with distinctly different compositions: bioactivity, viability of stem cells and antibiofilm effect against *Streptococcus mutans*, Mater. Sci. Eng. C 76 (2017) 233–241.
[31] A. Zamani, G.R. Omrani, M.M. Nasab, Lithium's effect on bone mineral density, Bone 44 (2009) 331–334.
[32] ISO Document 10993-5, Biological evaluation of medical devices, Tests for Cytotoxicity: In Vitro Methods, Part 5, International Organization for Standardization, Geneva, Switzerland, 2009.
[33] A.H. Cory, T.C. Owen, J.A. Barltrop, J.G. Cory, Use of an aqueous soluble tetrazolium/formazan assay for cell growth assays in culture, Cancer Commun. 3 (1991) 207–212.
[34] F.C. Serbena, I. Mathias, C.E. Foerster, E.D. Zanotto, Crystallization toughening of a model glass-ceramic, Acta Mater. 86 (2015) 216–228.
[35] W. Höland, V. Rheinberger, E. Apel, C. Hoen, Principles and phenomena of bioengineering with glass-ceramics for dental restoration, J. Eur. Ceram. Soc. 27 (2007) 1521–1526.
[36] M. Tylkowski, D.S. Brauer, Mixed alkali effects in Bioglass® 45S5, J. Non-Cryst. Solids 376 (2013) 175–181.
[37] I. Rehman, L.L. Hench, W. Bonfield, R. Smith, Analysis of surface-layers on bioactive glasses, Biomaterials 15 (1994) 865–870.
[38] C. Dueé, I. Grattepanche-Lebecq, F. Désanglois, C. Follet-Houttemane, F. Chai, H.F. Hildebrand, Predicting bioactive properties of phosphosilicate glasses using mixtures designs, J. Non-Cryst. Solids 362 (2013) 47–55.
[39] L.L. Hench, R.J. Splinter, W.C. Allen, T.K. Greenlee Jr., Bonding mechanisms at the interface of ceramic prosthetic materials, J. Biomed. Mater. Res. 2 (1) (1971) 117–141.
[40] L.L. Hench, Bioglass: 10 milestones from concept to commerce, J. Non-Cryst. Solids 432 (2016) 2–8.
[41] P. Ducheyne, J. Lemons, Bioceramics: materials characteristics versus in vivo behaviour, Ann. N. Y. Acad. Sci. 523 (1988).
[42] A.A. Ahmed, Leaching of some lithium silicate glasses and glass-ceramics by HCl, J. Non-Cryst. Solids 41 (1980) 57–70.
[43] F. He, J. Zhang, F. Yang, J. Zhu, X. Tian, X. Chen, In vitro degradation and cell response of calcium carbonate composite ceramic in comparison with other synthetic bone substitute materials, Mater. Sci. Eng. C50 (2015) 257–265.
[44] L.C. Junqueira, J. Carneiro, Histologia Básica, 10ª edição, Guanabara Koogan, Rio de Janeiro, 2004, p. 488.
[45] J. Moura, L.N. Teixeira, C. Ravagnani, O. Peitl, E.D. Zanotto, M.M. Beloti, H. Panzeri, A.L. Rosa, P.T. Oliveira, In vitro osteogenesis on a highly bioactive glass-ceramic (biosilicate), J. Biomed. Mater. Res. 82A (2007) 545–557.
[46] C. Capuccini, P. Torricelli, F. Sima, E. Boanini, C. Ristoscu, B. Bracci, G. Socol, M. Fini, I.N. Mihailescu, A. Bigi, Strontium-substituted hydroxyapatite coatings synthesized by pulsed-laser deposition: in vitro osteoblast and osteoclast response, Biomaterials 4 (2008) 1885–1893.
[47] E. Gentleman, Y.C. Fredholm, G. Jell, N. Lotfibakhshaiesh, M.D. O'Donnell, R.G. Hill, M.M. Stevens, The effects of strontium-substituted bioactive glasses on osteoblasts and osteoclasts in vitro, Biomaterials (14) (2010) 3949–3956.
[48] H. Zreiqat, Y. Ramaswamy, C. Wu, A. Paschalidis, Z. Lu, B. James, The incorporation of strontium and zinc into a calcium silicon ceramic for bone tissue engineering, Biomaterials 31 (2010) 3175–3184.
[49] G. Lusvardi, D. Zaffe, L. Menabue, C. Bertoldi, G. Malavasi, U. Consolo, In vitro and in vivo behaviour of zinc-doped phosphosilicate glasses, Acta Biomater. 5 (2009) 419–428.
[50] E. Ferensztajn-Rochowiak, J.K. Rybakowski, The effect of lithium on hematopoietic, mesenchymal and neural stem cells, Pharmacol. Rep. 68 (2016) 224–230.